Supplementary Figure 1
Lysophosphatidic acid acyl transferase (LPAAT) activities

LPAAT activity assay. Samples of lysates or purified proteins (5 or 10 µg) were inclubated with radiolabelled oleoyl-CoA labelled on the acyl chain and LPA for the times indicated (see methods for moree details). Samples were spotted on K60 silica gel chromatography plates (Merck) and run in chloroform:methanol:acetone:acetic acid:water, 50:20:10:10:5 followed by autoradiography.

a-c. Examples of TLC plates exposed for ^{14}C.

d,e. Coomassie staining of gels showing protein purifications. The endophilin N-BAR-His purification is not effective as there are still many contaminating bands, but the GST purification works well, and in the Coomassie gel we show this lane vastly overloaded to show up the residual protein contaminants.

f. Gel filtration trace and coomassie staining of fractions from dynamin double PH domain protein

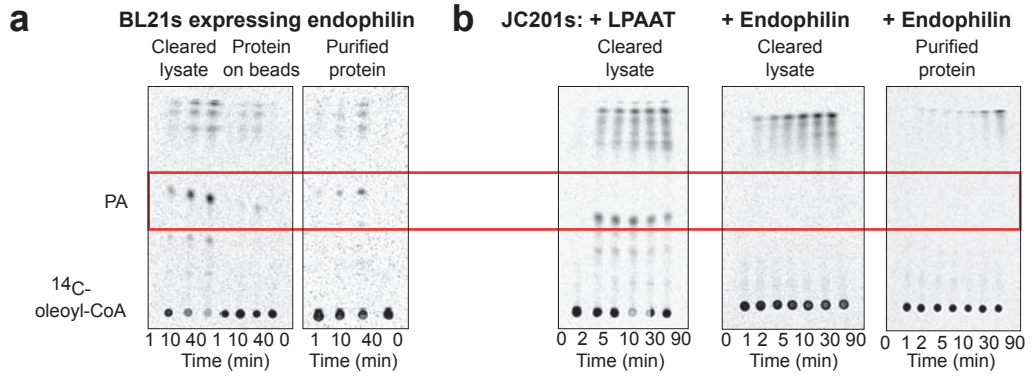

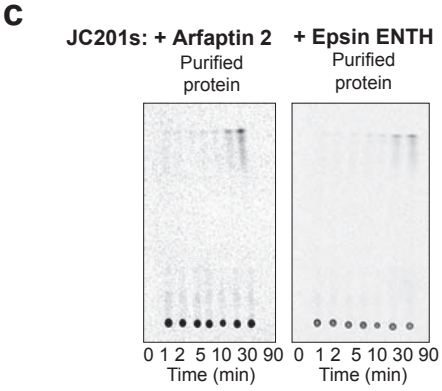

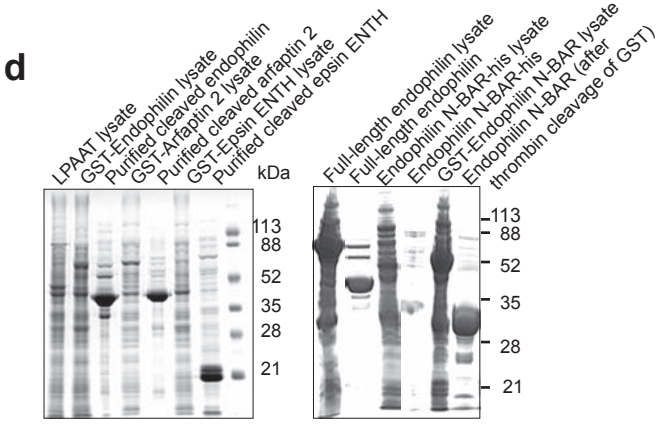

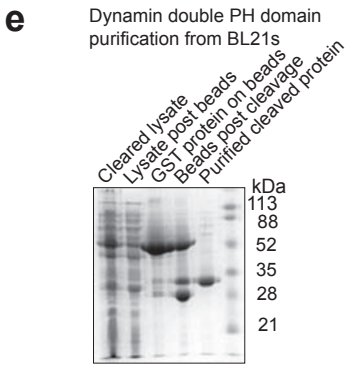

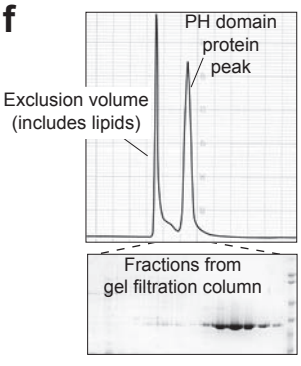

Supplementary Figure 2
Growth kinetics for JC201 bacteria expressing various endophilins and controls

a

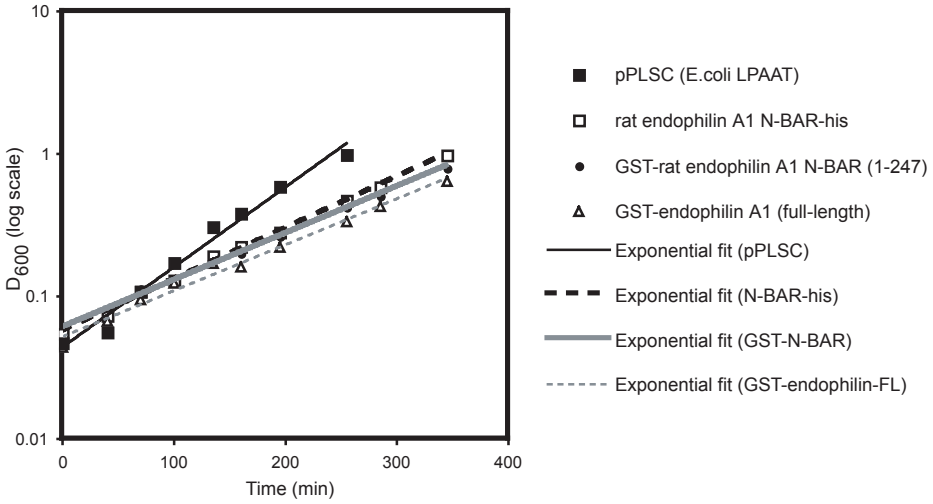

b

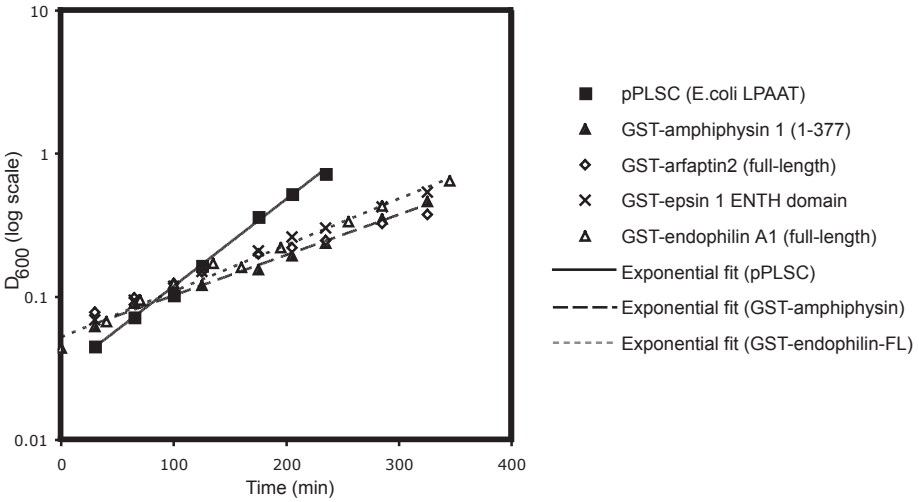

c

	Doubling time (min)		
Protein	**Mean**	**n**	**Std dev.**
LPAAT	54	4	2
GST-endophilin A1 N-BAR	94	2	7
endophilin A1 N-BAR-his	86	2	1
GST-endophilin A1 (FL)	89	2	6
GST-amphiphysin 1 (1-377)	97	2	13
GST-arfaptin 2 (FL)	115	2	23
GST-epsin 1 ENTH domain	97	2	4

Transformation of JC201 bacteria with endophilin does not lead to an acceleration of growth kinetics, unlike transformation of the endogenous LPAAT. **a**, Growth kinetics at 30^{o}C in LB medium for endophilin constructs. **b**, Growth kinetics at 30^{o}C in LB medium for control proteins compared to endophilin A1 and the E.coli LPAAT. **c**, Mean doubling times.

Supplementary Figure 3
Binding of endophilin to C16-CoA agarose

In support of their LPAAT hypothesis Schmidt and colleagues reported binding to LPAAT substrate palmitoyl-CoA linked to agarose. We show that this also occurs with other BAR domains and epsin but not with all control proteins. We wondered whether palmitoyl-CoA was binding at the BAR domain dimer interface. On analytical ultracentrifugation we find no evidence for disruption of dimerisation in the presence of palmtoyl-CoA and instead find that large aggregates are formed with both endophilin and control protein epsin ENTH domain. We also find no binding of CoA as would be expected of an LPAAT (Supplemental Fig. 4) and conclude that binding of palmitoyl-CoA is via the acyl chain and thus is unlikely to be at a transferase active site.

a, Binding to palmitoyl-CoA agarose is not restricted to LPAATs, a common attribute of membrane-trafficking, lipid-binding proteins. Sedimentation assays had 50 µl palmitoyl-CoA slurry (Sigma) in a 100 µl volume with 30 µg proteins and were washed twice with 150 mM NaCl, 20 mM HEPES pH 7.4, 2 mM DTT after 20 min incubation at 4 °C. Pellet (P) and supernatant (S) were resuspended in sample buffer and subjected to SDS-PAGE. **b,** Competition assays with acyl-CoAs show binding is via the acyl chain. Method as above except 30 µl of beads were used to reveal subtle effects; acyl-CoAs (Sigma) were used at 4 mM.

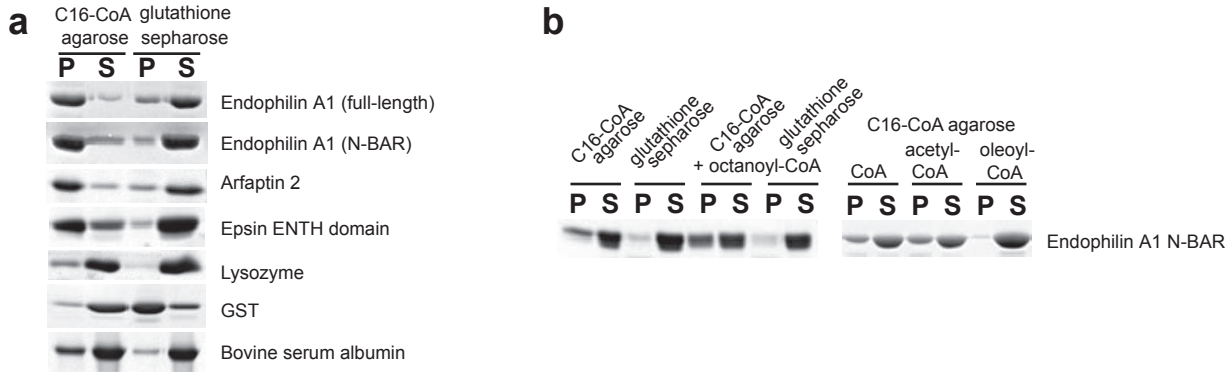

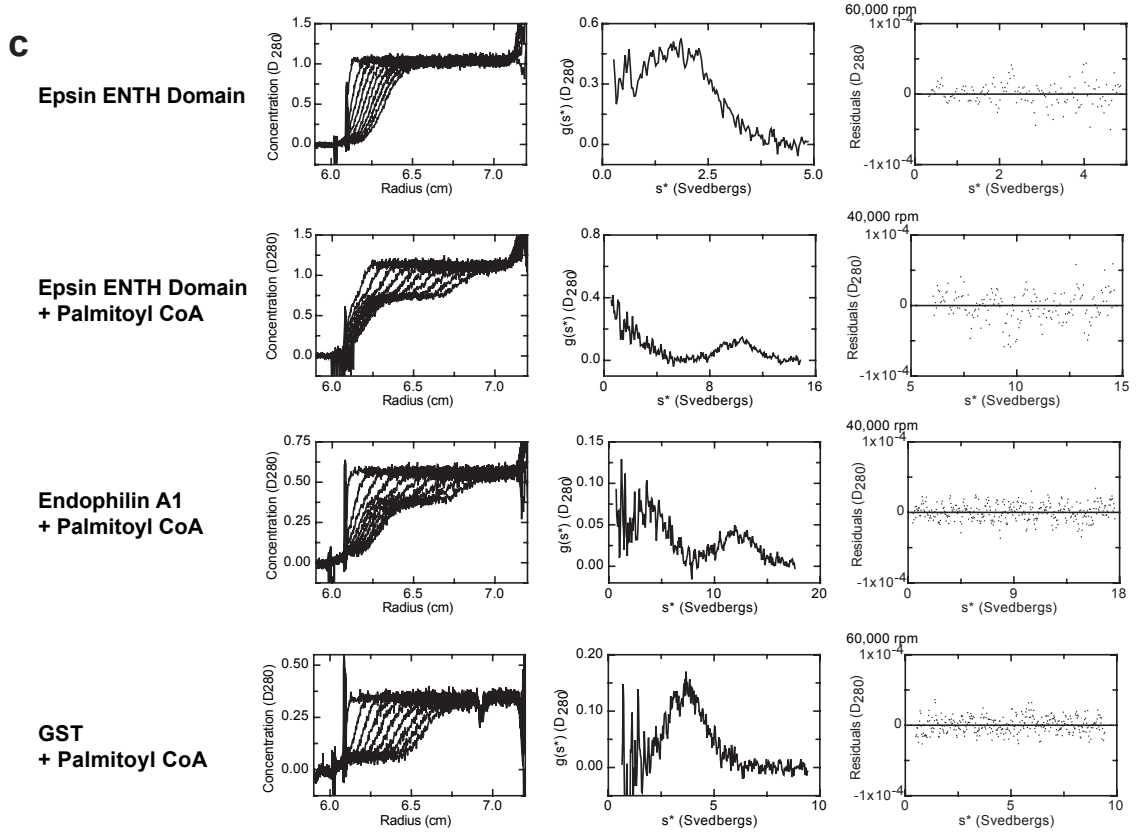

c, Velocity ultracentrifugation in the presence of endophilin A1 and palmitoyl-CoA. Two boundaries are observed for epsin1 ENTH domain and for endophilin in the presence of palmitoyl-CoA. The faster-moving boundary fits as an aggregate of ~150 kDa but the peak is broad which could reflect heterogeneous size. No regular arrays were observed by electron microscopy using 5% uranyl acetate negative stain (not shown). Analytical ultracentrifugation for endophilin is further described in Gallop et al (manuscript submitted). All components were at 30 µM in 150 mM NaCl, 20 mM HEPES pH 7.4, 2 mM DTT except GST which was at 12 µM. Sedimentation velocity runs were performed at the speeds indicated using a single cell and taking scans as quickly as possible. Data were analysed initially by plotting g(s*) against s*, where g(s*) is the fraction of material sedimenting between s* and (s*+δs*) using the DCDT+ software package (Version 1.05). This software was also used for the direct fitting of simple gaussian functions to dc/dt versus s curves to test for the number of components and estimate their molecular mass. Partial specific volumes and solvent densities were calculated as previously described in Peter et al. (2004) For the plots above, every tenth scan was taken to give visual separation of the traces.

Peter, B. J. et al. *Science* **303,** 495-499 (2004).

Supplementary Figure 4

Endophilin A1 does not bind CoA

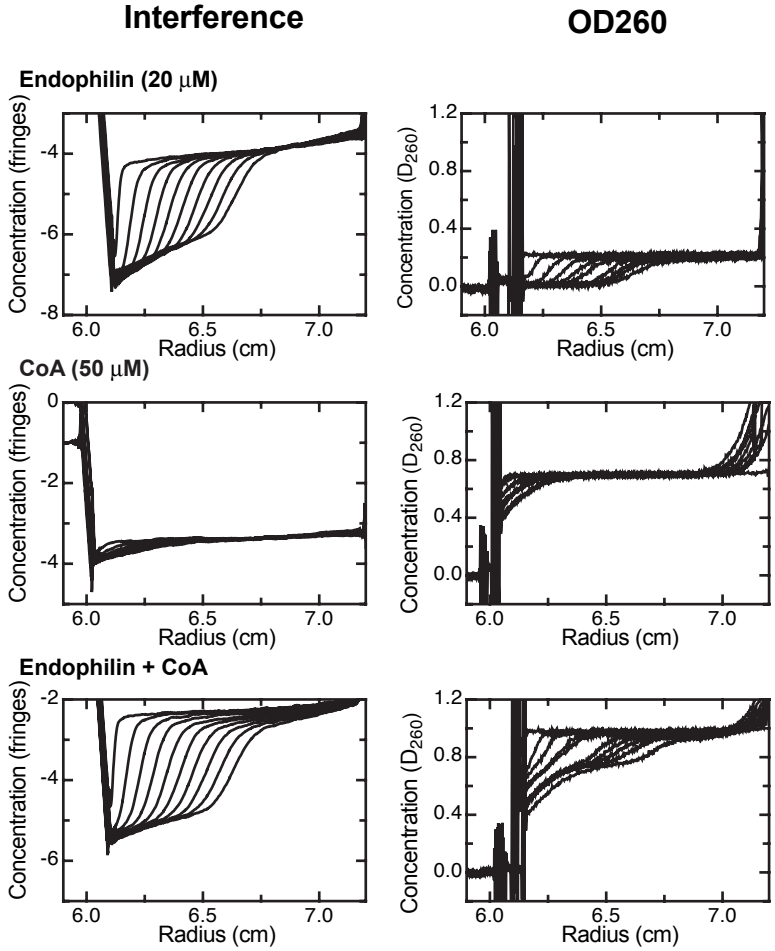

Quantitative analysis (dc/dt):

	Interference	D_{260}
$s_{20,w}$	3.8S	3.9S
concentration	1.9 fringes	0.2
$s_{20,w}$		0.5S
concentration		0.66
$s_{20,w}$	3.8S	3.9S
concentration	2.4 fringes	0.2
$s_{20,w}$		0.8S
concentration		0.4

Velocity ultracentrifugation in the presence of endophilin A1 and CoA. The presence of CoA does not affect the sedimentation (i.e. oligomerisation state) of endophilin, seen in the interference traces, and there is no evidence for CoA co-sedimenting with endophilin (comparison of OD260 traces). Runs were performed at 4℃ in 150 mM NaCl, 20 mM Tris pH 7.4, 0.5 mM TCEP at the concentrations indicated. For calculation methods, see Supplementary Fig. 3.

Endophilin A1 binding to liposomes

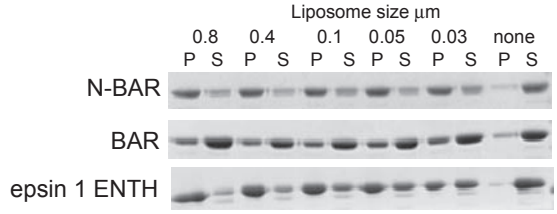

Endophilin BAR domain binding is sensitive to the size of the liposomes and binds better to liposomes of higher curvature (smaller ones). N-BAR and epsin binding are independent of liposome size in this assay consistent with the presence of an amphipathic helix.

Liposome sedimentation assays were performed with 0.2 mg/ml Folch liposomes. For curvature sensing assays, liposomes were made in 150mM NaCl, 20 mM HEPES pH 7.4, 2 mM DTT and filtered to appropriate size. 2 μM endophilins and 15 μg epsin were incubated in a volume of 100 μl for 10 mins and sedimented at 100,000 g. Sample buffer was added to the pellet (P) and supernatant (S) and equivalent quantities run on SDS-PAGE and stained with Coomassie brilliant blue.

Supplementary Figure 5
NADH binds to CtBP but does not compete with LPAAT activity

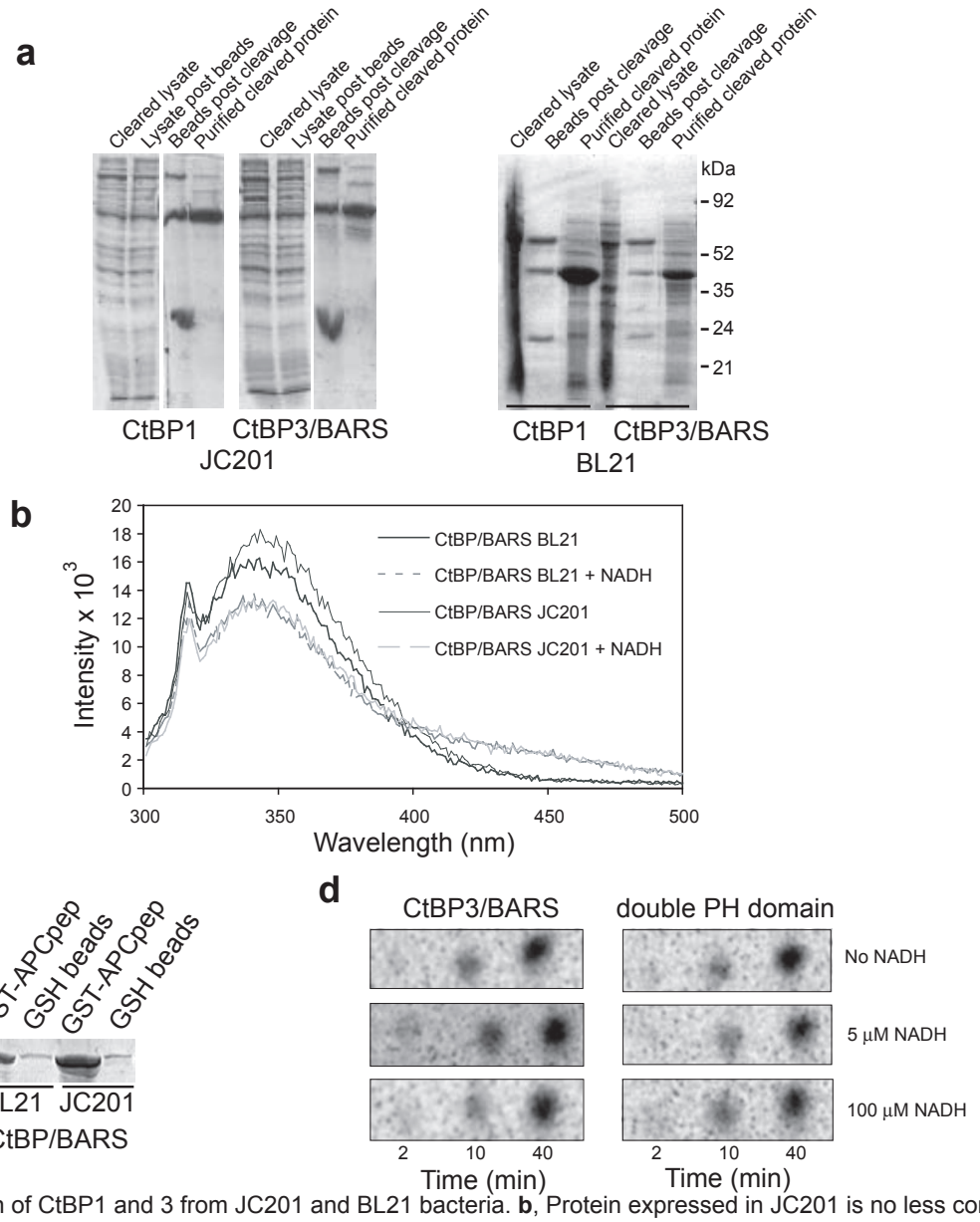

a, Protein purification of CtBP1 and 3 from JC201 and BL21 bacteria. **b**, Protein expressed in JC201 is no less competent than BL21 protein at binding NADH. **c**, Protein expressed in JC201 or BL21 bacteria is competent to interact with CtBP binding sequence present in adenomatous polyposis coli (APC). The APC fragment used has 2 PxDLS motifs and has previously been reported to bind CtBP1 (Hamada and Bienz 2004). **d**, Nardini et al. report that CtBP3/BARS binds to oleoyl-CoA with an affinity of 5 μM at the same binding site as NADH (which has an affinity of 100 nM), and model the binding of CoA into their structure. We see no inhibition at 10-fold excess NADH levels over oleoyl-CoA, contrary to what would be expected of intrinsic CtBP3/BARS LPAAT activity. The authors also suggest that an oligomeric change may be required for LPAAT activity to take place as the acyl chain of the acyl-CoA substrate would clash with the dimer interface. We find that there is no change in the oligomeric state of CtBP in the presence of oleoyl-CoA, as shown by analytical ultracentrifugation (Supplementary Fig. 6). We suggest that the activity is again a co-purification artefact. Although reported to bind NADH competitively with oleoyl-CoA, NADH, which binds with 50-fold higher affinity, does not inhibit the LPAAT activity of CtBP3/BARS or control artefact LPAAT activity of dynamin 2xPH domain.

NADH binding was detected using a fluorescence resonance energy transfer based assay described by Fjeld et al. These measurements were made on the Fluoromax 2 fluorimeter (Spectra) with an excitation wavelength of 285 nm and collecting an emission spectrum from 300 - 500 nm with the proteins and NADH at a 500 nM concentration. The result shown is for CtBP1, similar results were obtained for CtBP3/BARS.

Pulldown assay – proteins were incubated for 40 min at 4 C with bead bound GST-APC(488-597), washed twice and run on SDS-PAGE (the result shown is CtBP3/BARS).

Fjeld, C. C., Birdsong, W. T. & Goodman, R. H. Differential binding of NAD+ and NADH allows the transcriptional corepressor carboxyl-terminal binding protein to serve as a metabolic sensor. *Proc Natl Acad Sci U S A* **100,** 9202-9207 (2003).

Nardini, M., Spano, S., Cericola, C., Pesce, A., Massaro, A., Millo, E., Luini, A., Corda, D., Bolognesi, M. CtBP/BARS: a dual-function protein involved in transcription co-repression and Golgi membrane fission. *EMBO J* **22** 3122-3130 (2003).

Hamada, F. & Bienz, M. The APC tumor suppressor binds to C-terminal binding protein to divert nuclear beta-catenin from TCF. *Dev Cell* **7,** 677-685 (2004).

Supplementary Figure 6
Oligomerisation of CtBP is unaffected by Oleoyl-CoA

CtBP alone (30 μM)

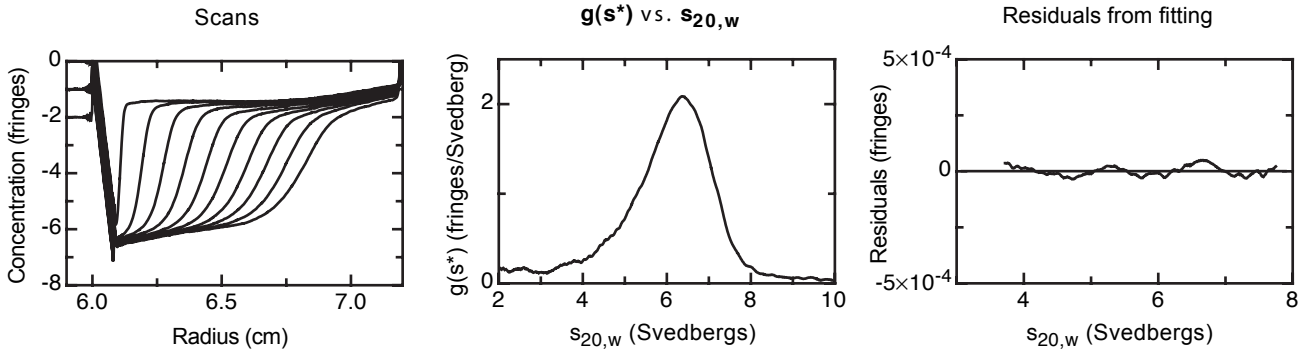

CtBP + Oleoyl-CoA (90 μM)

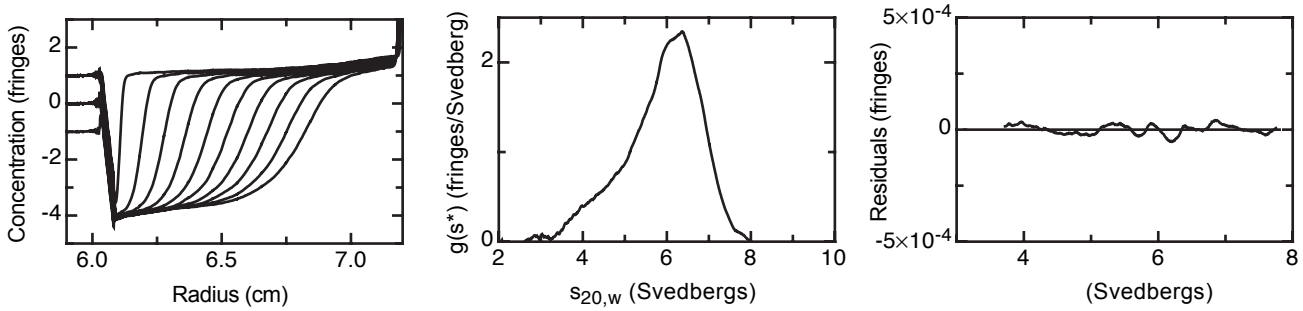

	CtBP alone	CtBP + Oleoyl-CoA
$S_{20,w}$ 1 (Svedbergs)	5.4 (±0.04)	5.4 (±0.03)
Concentration 1 (fringes)	1.6 (±0.06)	1.6 (±0.06)
Molecular mass 1 (kDa)	35 (±0.9)	36 (±0.8)
$S_{20,w}$ 2 (Svedbergs)	6.3 (±0.01)	6.3 (±0.01)
Concentration 2 (fringes)	2.6 (±0.06)	2.6 (±0.06)
Molecular mass 2 (kDa)	105 (±1)	106 (±1)

Velocity ultracentrifugation in the presence CtBP3/BARS and oleoyl-CoA. The presence of oleoyl-CoA does not affect the sedimentation (i.e. oligomerisation state) of CtBP3/BARS seen in the interference traces. Runs were performed at 4°C in 150 mM NaCl, 20 mM Tris pH 7.4, 0.5 mM TCEP at the concentrations indicated. For calculation methods, see Supplementary Fig. 3.